

Direct Observation and Hole Burning of the Lowest Exciton Level (B870) of the LH2 Antenna Complex of *Rhodopseudomonas acidophila* (Strain 10050)

H.-M. Wu, N. R. S. Reddy, and G. J. Small*

Ames Laboratory—USDOE and Department of Chemistry, Iowa State University, Ames, Iowa 50011

Received: September 10, 1996; In Final Form: November 4, 1996[®]

Results of 4.2 K absorption and hole-burning experiments on the B850 absorption band of isolated LH2 (B800–850) complexes from *Rhodopseudomonas acidophila* are presented for samples that exhibited a B850 absorption band of sufficient narrowness (200 cm^{-1}) to allow for direct observation of the lowest exciton level of the B850 ring of dimers as a weak but distinct shoulder at the red edge of the B850 band. This shoulder correlates perfectly with the zero-phonon hole action spectrum of B870 which has been assigned as the lowest exciton level of B850. The action spectrum reveals that the B870 band carries an inhomogeneous width of $120 \pm 10\text{ cm}^{-1}$, is characterized by weak electron–phonon coupling, and carries 3% of the total intensity of the B850 absorption band. The B870 exciton level lies 200 cm^{-1} below the B850 band maximum. Based on the X-ray structure of LH2 and under the assumption of perfect C_9 symmetry (absence of diagonal and/or off-diagonal energy disorder) for the B850 ring, the B850 maximum should be determined by the strongly allowed E_1 level of the C_9 -array of bacteriochlorophyll *a* dimers and B870 (the A level) should be adjacent, forbidden in absorption and the lowest energy level. However, the location of the A level 200 cm^{-1} below the E_1 level appears to require a coupling between the nearest bacteriochlorophyll *a* monomers of adjacent dimers that is larger than the coupling between the monomers of the special pair of the reaction center of *Rhodobacter sphaeroides*. As a result, it is concluded that diagonal and/or off-diagonal energy disorder within the B850 ring must be taken into account in order to understand B870 and the Q_y electronic structure of B850. However, the temperature dependence (4.2–270 K) of the LH2 absorption spectrum reveals that the coupling between neighboring B850 molecules strengthens upon formation of the glycerol:H₂O glass near 150 K. This is important for electronic structure calculations that utilize the room temperature structure of LH2 and low-temperature spectroscopic data. Finally, data pertaining to the pure dephasing of the B870 exciton level are presented and interpreted in terms of scattering due to imperfections in the B850 ring.

Introduction

The Q_y electronic structure and excitation energy transfer dynamics of the LH1 and LH2 antenna complexes of purple bacteria have long been subjects of much interest. (For a recent review see Sundström and van Grondelle.¹) LH2 and LH1 are respectively distal and proximal to the reaction center and in *Rhodobacter sphaeroides* and *Rhodopseudomonas acidophila* (strain 10050) are also referred to as B800–850 and B875, respectively, because of the location (in nanometers) of their bacteriochlorophyll *a* (BChl *a*) absorption band maxima at room temperature. Structural models for LH1 and LH2 put forth during the middle to late 1980s have in common an α,β polypeptide pair that binds two BChl *a* molecules at the periplasmic side of the membrane and, in the case of LH2, one BChl *a* at the cytoplasmic side. (See ref 2 for a recent review.) It was generally believed that some type of cyclic arrangement of α,β pairs constituted the unit cell of the two complexes with the BChl *a* molecules at the periplasmic side responsible for the B850 and B875 absorption bands of LH2 and LH1, respectively, the BChl *a* molecules bound at the cytoplasmic side being responsible for B800 of LH2.

Recently, the X-ray structure of the LH2 complex of *Rps. acidophila* (strain 10050) was reported at a resolution of 2.5 Å .^{3,4} The structure revealed that this complex is a cyclic 9-mer of α,β pairs. The arrangement of the BChl *a* molecules is shown in Figure 1⁵ where the arrows, which lie nearly in the membrane plane, indicate the direction of Q_y transition dipoles. Several Mg···Mg separation distances are indicated. The relatively large

separation of 21 Å between adjacent B800 molecules results in weak coupling, $V \sim 20\text{ cm}^{-1}$,^{5,6} consistent with hole-burning data which indicated that excitonic effects should be unimportant for the B800 ring.⁶ However, the B850 nearest-neighbor distances of 8.9 and 9.6 Å lead to large coupling energies, $V \sim 300\text{ cm}^{-1}$.⁵ Thus, and as deduced on the basis of hole burning data,⁷ exciton level structure is expected to be important for understanding the nature of the B850 absorption band and, for example, the B800 \rightarrow B850 energy transfer process.^{6–8} Figure 1 reveals that the B850 ring of 18 BChl *a* molecules should be viewed as a 9-mer of dimers. There are, however, two choices for the basic dimer, one associated with the 8.9 Å separation distance and the other with the distance of 9.6 Å, (Figure 1); the choice of dimer is quite arbitrary, although, from a symmetry point of view, the 9.6 Å dimer is the correct choice. Irrespective of the choice, the Q_y transition dipoles of the two monomers are close to being antiparallel. Since the interaction energy between the monomers is positive, only the lower dimer component (l) carries significant absorption intensity as can be deduced⁶ on the basis of the structural information provided in the first paper on the structure of LH2.³ When interactions between dimers are taken into account, these two levels (l and u) spawn two bands of exciton levels, all but one of which levels are doubly degenerate under perfect C_9 symmetry; cf. Figure 2. Concerning B875, moderate resolution electron diffraction data indicate that it is a cyclic 16-mer of BChl *a* dimers.⁹ (The inner diameter of the B875 ring appears to be large enough to house the reaction center.) High-pressure studies of the B800, B850, and B875 bands of *Rb. sphaeroides*⁶ led to the conclusion that the coupling between nearest-neighbor monomers of B875

[®] Abstract published in *Advance ACS Abstracts*, January 1, 1997.

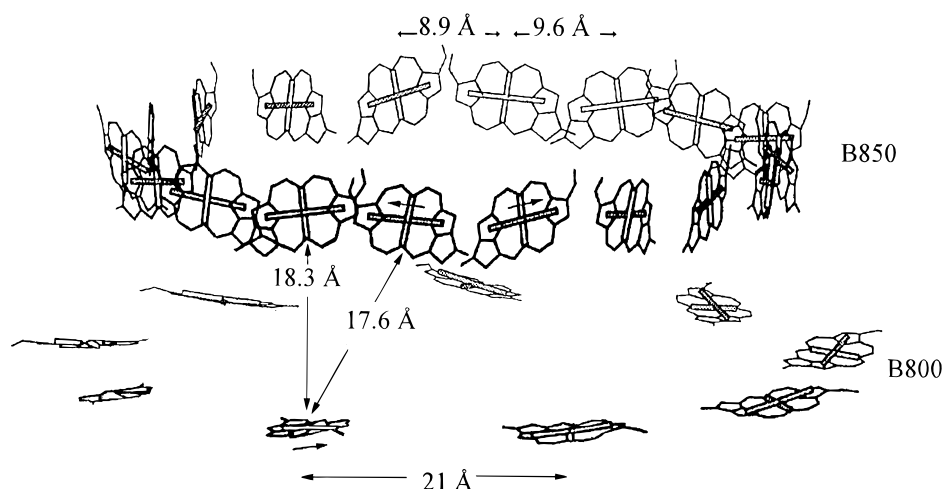


Figure 1. A schematic (based on Figure 1 in ref 5) showing the arrangement of the 18 B850 (upper ring) and nine B800 (lower ring) molecules in the LH2 antenna complex from *Rps. acidophila*. Within the circular array, nearest-neighbor distances (Mg...Mg) between B850 molecules are either 8.9 or 9.6 Å. The 9.6 Å distance is that of the two BChl *a* molecules associated with the α,β polypeptide pair. The two B850 BChl *a* molecules nearest to a B800 molecule are separated by distances of 17.6 and 18.3 Å. The horizontal arrows indicate the directions of the Q_y transition dipoles.

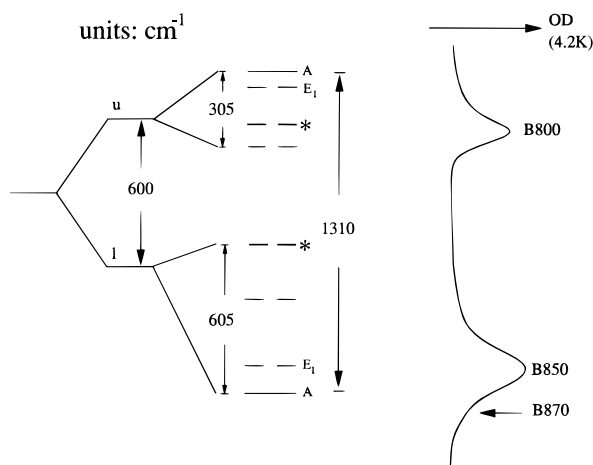


Figure 2. The 4.2 K absorption spectrum of the LH2 complex from *Rps. acidophila* is shown together with the calculated exciton manifold of the B850 ring (see text). u and l refer to the upper and lower components of the basic B850 dimer. The 9-fold symmetry of the dimers within the structural subunit leads to the exciton manifolds shown. The unit of the numbers shown is cm^{-1} . The lowest energy level of the l-manifold is $j = 0$ (A) followed next by the strongly absorbing $j = \{1,8\}$ (E_1) level which has been placed at the B850 absorption maximum. The asterisks indicate two closely spaced doubly degenerate levels.

is stronger than in B850. Thus, exciton level structure can also be expected to be important for understanding the nature of the B875 absorption band.

Here we present low-temperature absorption and persistent nonphotochemical hole-burning data on the B800–850 complex from *Rps. acidophila* obtained with a sample that yielded 4.2 K absorption bandwidth of unprecedented narrowness. The reduction in bandwidth of B850 allowed for direct observation of the weakly absorbing B870 component which lies at the red edge of the B850 absorption band. Zero-phonon hole action spectroscopy¹⁰ is used to determine the position, intensity, and inhomogeneous broadening of the B870 band as well as the dephasing time of the B870 exciton level. Zero-phonon hole action spectra had previously been used to identify B870 (as well as its B875 counterpart, B896) in *Rb. sphaeroides*¹⁰ and *Rps. acidophila*¹¹ but with samples whose absorption bandwidths were too broad to permit direct observation of B870. In these works, both B850 and B875 were found to exhibit significant homogeneous broadening, $\Gamma_h \sim 200 \text{ cm}^{-1}$. This broadening

was attributed to exciton level structure and ultrafast interexciton level relaxation processes. (Because of the possibility that more than one exciton level may contribute absorption intensity to B850, one should not use $\Gamma_h \sim 200 \text{ cm}^{-1}$ to arrive at a time for relaxation between a pair of exciton levels. Nevertheless, the results of refs 10 and 11 indicate interexciton level relaxations occur on a time scale of about 100 fs.) The results of subsequent femtosecond experiments^{12,13} and the X-ray structure of the B800–850 complex are consistent with this interpretation. On the basis of the observed satellite hole structure obtained by selective burning of B870 and B896, Reddy et al.¹⁰ favored the interpretation that has both of them being the lowest exciton level of B850 and B875, respectively, although they pointed out that energy disorder associated with the Q_y energies of and intermolecular interactions of the cyclic ring structures might lead to a low-lying state that is quite highly localized on a single dimer. The data presented in the present paper and the X-ray structure of LH2 of *Rps. acidophila* are used to explore in greater detail the nature of B870 since its understanding is important for elucidation of the Q_y electronic structure of the LH2 complex. An important consequence of the analysis is that the assignment of B870 (which lies 200 cm^{-1} to lower energy of the B850 absorption maximum) as the lowest exciton level (A) of B850 is problematic *under* the assumption of perfect C_9 symmetry, i.e., in the absence of diagonal and/or off-diagonal energy disorder which serves to destroy the symmetry. It is concluded that consideration of such disorder (structural heterogeneity) within B850 rings is important for understanding B870. Temperature-dependent absorption data are presented which establish that BChl *a*–BChl *a* excitonic coupling within the B850 ring weakens at temperatures $\geq 150 \text{ K}$ (approximately glass transition temperature of the glycerol: H_2O glass used). This finding is important to theoretical modeling of B850's excited state electronic structure based on the room temperature X-ray structure and low-temperature spectroscopic data. The thermal broadening of the B850 band is noted to be qualitatively consistent with the dephasing being due to downward interexciton level relaxation by one-phonon emission.

Experimental Section

Isolated B800–850 complexes of *Rps. acidophila* (strain 10050) were prepared as described in ref 14. The isolation procedure was the same as that used in the work that led to the

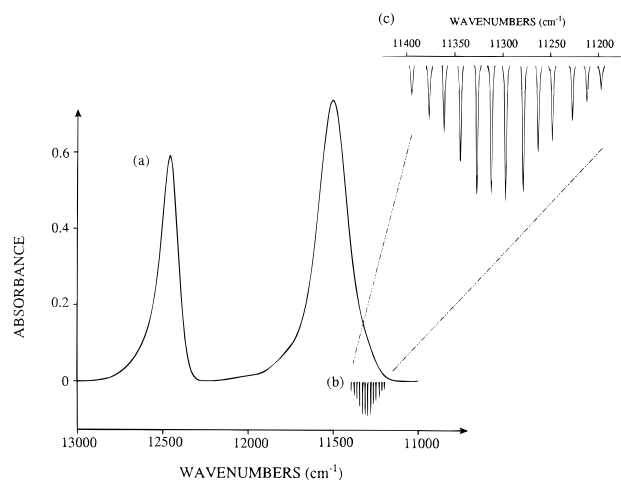


Figure 3. (a) The 4.2 K absorption spectrum of LH2 complex from *Rps. acidophila*. The B800 band at 12457 cm^{-1} has a width of 120 cm^{-1} , while the B850 band at 11 503 cm^{-1} has a width of 200 cm^{-1} . (b) The zero-phonon hole action spectrum (arbitrary units) of B870 was generated with a constant burn fluence of 100 J/cm^2 at 11 wavelengths ranging from 11 197 to 11 395 cm^{-1} . Order of burning was from high to low energy so as to minimize light-induced hole filling. There was no temperature cycling between burns. (c) An expanded view of (b). The envelope of the action spectrum of B870 centered at 11 300 cm^{-1} carries a width of $120 \pm 10 \text{ cm}^{-1}$.

X-ray structure.^{3,4} The samples used were from the same batch as used in our recent high-pressure hole-burning studies of the B800 \rightarrow B850 energy transfer process.⁸ The sample used in the present work yielded 4.2 K B800 and B850 absorption bandwidths of 125 and 200 cm^{-1} which are narrower by 5 and 20 cm^{-1} than those reported in ref 8. We have no explanation for the narrowing effect but note that the original batch was divided into samples suitable for single experiments and that they were stored in the dark at 200 K over several months. We hasten to add, however, that the results reported here for B870 were confirmed for other samples from this batch; i.e., slight variations in the B850 width of $\sim 20 \text{ cm}^{-1}$ had a negligible effect on B870's energy, width, and intensity. We consider the narrow widths of the LH2 absorption bands to be indicative of high sample quality.

A Janis 8-DT convection cooling liquid helium cryostat was used. B800–850 complexes were dissolved in a glycerol:water (2:1 by volume) glass-forming mixture. 0.1% LDAO detergent was added for solubilization. The hole-burning apparatus is described in ref 15. Briefly, a Bruker HR 120 Fourier transform spectrometer was used for recording of preburn and postburn absorption spectra, the difference of such spectra being the persistent nonphotochemical hole-burned spectrum. All spectra reported were obtained after a 100 scan average at a resolution of 1 cm^{-1} . The zero-phonon holes (fractional depth ≤ 0.15) burned into B870 in order to determine the dephasing time of the B870 exciton level were measured at a resolution of 0.5 cm^{-1} . The burn laser was a Coherent CR 899-21 Ti:sapphire laser (line width 0.07 cm^{-1}) pumped by a 15 W Innova Ar ion laser. Burn intensities and times are given in the figure captions.

Results and Discussion

Figure 3 shows the 4.2 K absorption spectrum of the isolated B800–850 complex of *Rps. acidophila*. The widths of the B800 and B850 bands, located at 802.9 and 869.6 nm, are 125 and 200 cm^{-1} , respectively. Inspection of the low-energy tail of B850 reveals a weak but distinct shoulder; it is more apparent in Figure 4. Indicated in the region of the shoulder in Figure 3 are a series of zero-phonon holes (ZPH) burned with a fixed laser fluence at 4.2 K. An expanded view of this ZPH hole

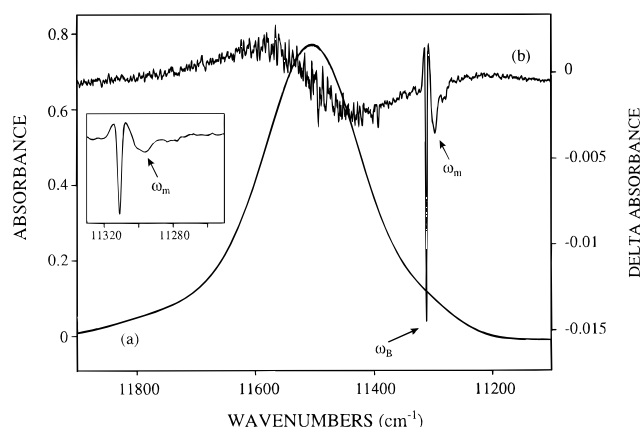


Figure 4. (a) The 4.2 K absorption spectrum of LH2 from *Rps. acidophila* showing the B850 band. A 4.2 K hole-burned spectrum (b) obtained by burning close to the maximum of the B870 band (11 311 cm^{-1} , burn intensity = 160 mW/cm^2 and burn time = 120 s) shows, in addition to a ZPH at the burn frequency, a pseudo-phonon sideband hole 16 cm^{-1} to lower energy of the ZPH and a broad B850 satellite hole, see text. The inset shows an expanded view of the ZPH with a width of $1.9 \pm 0.2 \text{ cm}^{-1}$ (read resolution of 0.5 cm^{-1}).

action spectrum is shown in the upper right-hand corner. For clarity, the weak phonon sideband holes associated with the ZPH have been deleted. The fractional hole depths of the most intense holes are ~ 0.15 . The contour of the ZPHs is centered at $11\,300 \pm 10 \text{ cm}^{-1}$ ($885.0 \pm 0.8 \text{ nm}$), which is 200 cm^{-1} lower in energy than the B850 absorption maximum. The inhomogeneous width of the contour is $120 \pm 10 \text{ cm}^{-1}$. The ZPH action spectrum represents the B870 absorption profile. The just-stated results are in quite close agreement with those reported earlier.¹¹ However, Figure 3 shows, for the first time, that the ZPH action spectrum correlates with a weak but distinct absorption feature at the red edge of the B850 band. In earlier hole-burning studies of B850 of *Rb. sphaeroides*⁷ and *Rps. acidophila*,¹¹ it was found that burn frequencies located near and to higher energies of the B850 absorption maximum produced only a very broad hole (bleach) in B850. This proved that the B850 band suffers from very significant homogeneous broadening, $\sim 200 \text{ cm}^{-1}$ for *Rb. sphaeroides*. A large contribution from homogeneous broadening for the sample used in the present study was confirmed (results not shown). As mentioned in the Introduction, the homogeneous broadening was attributed to exciton level structure and interexciton level relaxation associated with the main part of the B850 band.

Figure 4 shows a persistent nonphotochemical hole-burned spectrum obtained with a burn frequency $\omega_B = 11\,311 \text{ cm}^{-1}$ located near the peak of B870. Labeled as ω_m is the pseudo-phonon sideband hole which is displaced from the ZPH by 16 cm^{-1} . (The real phonon sideband hole on the blue side of the ZPH is not discernible because the electron–phonon coupling is weak and because of the interference from the broad satellite hole center at 11 450 cm^{-1} .) A value of 18 cm^{-1} was reported in ref 11 where the prominence of the ZPH over the phonon sideband hole in intensity also showed that the electron–phonon coupling for B870 is weak with a Huang–Rhys factor $S < 1$. In Figure 4, the ZPH is seen to suffer from interference from the antihole associated mainly with the pseudo-phonon sideband hole. Weak electron–phonon coupling, as measured by hole burning, is generally observed for antenna protein complexes in sharp contrast with the special pair of reaction center complexes. (For a recent discussion see ref 16.) The second point to be made from Figure 4 is that burning into B870 produces a broad satellite hole in the main part of B850 which is accompanied by a comparably broad blue-shifted antihole symptomatic of nonphotochemical hole burning of $\pi\pi^*$ states.¹⁷

Such satellite hole structure has been studied in considerable detail for *Rps. acidophila*¹¹ as well for B875 and B896 of *Rb. sphaeroides*.¹⁰ It is indicative of correlation between B870 and higher energy levels of B850 by virtue of the delocalized excitonic nature of the B850 ring states.^{10,11} Again, B896 is the counterpart of B870 for LH1 (B875).

High-resolution scans of ZPH burned into B870 yielded a hole width of $2.0 \pm 0.2 \text{ cm}^{-1}$ at 4.2 K. In a previous study, a value of 2.0 cm^{-1} was also obtained.¹¹ In that work the homogeneous broadening was attributed to pure dephasing associated with scattering of the B870 ring excitation with structural defects in the ring. A width of 2.0 cm^{-1} corresponds to a pure dephasing time of 5.3 ps. For B870 of LH2 of *Rb. sphaeroides* (NF57 strain), a dephasing time of 6.6 ps has been reported.¹⁰

Nature of B870 of LH2. The results shown in Figure 3 establish that B870 lies 200 cm^{-1} below the B850 absorption maximum and carries an inhomogeneous width of 120 cm^{-1} . In a previous study¹¹ of LH2 of *Rps. acidophila*, B870 was found to lie 270 cm^{-1} below the B850 maximum, but in that work the sample used exhibited a very large B850 absorption bandwidth of 430 cm^{-1} , over twice as large as the width shown in Figure 3. The present determination of 200 cm^{-1} is closer to the value of 250 cm^{-1} determined for LH2 samples from *Rb. sphaeroides* (NF57 mutant) which exhibited a B850 bandwidth of 280 cm^{-1} .⁷ Very recently, we used ZPH action spectroscopy to identify and characterize B870 in isolated LH2 complexes from *Rhodospirillum rubrum* (to be published) for which an X-ray structure also exists. The structure reveals that¹⁸ in this species LH2 is an 8-mer of α, β polypeptide pairs. It may be concluded that B870 is a general feature of purple bacteria that exhibit the B850 band, at least at cryogenic temperatures. That the X-ray structures reveal that LH2 of *Rps. acidophila* and *Rs. rubrum* is respectively a 9-mer and 8-mer of α, β polypeptide pairs is interesting. It is conceivable that the difference could be a consequence of the crystal growth procedures. More to the point for the present work is that one cannot state with certainty that the ensemble of isolated LH2 complexes studied was homogeneous, i.e., that all members were 9-mers. However, that the ensemble studied might have been say a mixture of 8-mers and 9-mers is of little consequence to the question of whether or not B870 lying 200 cm^{-1} below the B850 maximum and viewed as the lowest delocalized exciton level of the B850 ring is reasonable under the assumption of perfect C_9 -symmetry and the room temperature X-ray structure.

We have investigated this question theoretically. Details will be presented elsewhere in a paper primarily concerned with the effects of diagonal and off-diagonal energy disorder on the excitonic energies, wave functions, and dipole strengths of the B850 ring.¹⁹ Briefly, the nearest dimer–dimer coupling approximation was employed and the interaction between B800 and B850 molecules ignored. The calculations of Sauer et al.,⁵ which employ the point monopole method and take into account coupling between all BChl *a* molecules of LH2, indicate that these approximations are good enough to provide an informative picture of the B850 exciton level energies. As in their work, we chose the basic dimer of B850 to be that associated with the α, β polypeptide pair (Mg···Mg separation of 9.6 \AA). For evaluation of the nearest-neighbor dimer–dimer interaction, one requires four BChl *a*–BChl *a* coupling energies. These were determined using the results of Sauer et al., although slightly rounded off values were used since Sauer et al. assume that the symmetry inequivalent monomers of the dimer have identical Q_y energies and ignore electron-exchange interactions and because of the difficulty associated with treating dielectric screening. With reference to Figure 2, the monomer–monomer coupling of the basic dimer was set equal to $+300 \text{ cm}^{-1}$, which

is close to the value calculated by Sauer et al.⁵ Thus, the splitting between the upper (u) and lower (l) levels of the dimer is 600 cm^{-1} . It is then a simple matter to calculate the energetics of the ring-exciton manifolds which are spawned by u and l of the basic dimer since the delocalized wave functions are determined by symmetry and, with the nearest dimer–dimer coupling approximation, simple analytical expressions for the exciton level energies exist. (See, for example, ref 20.) Following generation of the two exciton manifolds, one needs to consider the interactions between u- and l-type levels. Only levels transforming like the same irreducible representation of the C_9 point group can mix. The resulting picture for the excitonic energies is shown in Figure 2 where one sees two energetically displaced manifolds with widths of 305 and 605 cm^{-1} . Under C_9 symmetry the irreducible reps are labeled by $j = 0, 1, \dots, 8$. The $j = 0$ (A) level is nondegenerate while the $j = \{1, 8\}$ (E_1), $\{2, 7\}$, $\{3, 6\}$, and $\{4, 5\}$ levels are doubly degenerate. For the l-manifold, the $j = 0$ level lies lowest followed next by the $j = \{1, 8\}$ and $j = \{2, 7\}$ degenerate levels. For the u-manifold, the $j = 0$ lies highest in energy followed next by the $j = \{1, 8\}$ level. Under cyclic symmetry and with the Q_y transition dipoles nearly perpendicular to the principal rotation axis, only one of the 10 exciton levels shown in Figure 2 carries significant absorption intensity or dipole strength. It is the $j = \{1, 8\}$ (E_1) level of the l-manifold, consistent with the calculations of Sauer et al.⁵ The exciton level energy diagram of the B850 ring given in Figure 2 is quite similar to that of Sauer et al.,⁵ with both showing that the u-manifold levels lie in the near vicinity of B800. Slight differences are to be expected since we have employed the nearest dimer–dimer coupling approximation and neglected B800–B850 molecular interactions. The extent to which differences between their and our results are significant remains to be determined, especially when energy disorder is taken into account.

With this brief discussion of the procedure used to generate the energy level diagram Figure 2, we come to the major point. It is that the lowest energy level of the l-manifold, the $j = 0$ level, lies only $\sim 100 \text{ cm}^{-1}$ below the $j = \{1, 8\}$ level which carries almost all of the dipole strength and, with perfect cyclic symmetry, determines the energy of the B850 absorption maximum. Sauer et al.⁵ also arrived at a value of 100 cm^{-1} . In our earlier work,¹¹ which preceded the X-ray structure of LH2 of *Rps. acidophila*, the interpretation for B870 favored was that it is the $j = 0$ level of the manifold of exciton levels associated with B850. The problem is that our results establish that B870 lies 200 cm^{-1} ($\pm 10 \text{ cm}^{-1}$) below the B850 maximum. To a reasonable approximation, the $j = 0$ level should be split off from the $j = \{1, 8\}$ level by $0.45|V|$ for C_9 symmetry. Here V is the effective coupling between neighboring dimers appropriate for the l-manifold. Thus, the observed splitting of 200 cm^{-1} requires that $|V| \sim 400 \text{ cm}^{-1}$, which, in turn, requires¹⁹ a coupling of $\sim 700 \text{ cm}^{-1}$ between closest BChl *a* molecules ($R_{\text{Mg}\cdots\text{Mg}} = 8.9 \text{ \AA}$) of nearest-neighbor dimers. Such a coupling is over twice as large as that calculated by Sauer et al.⁵ and as large as the coupling between the monomers of the special pair in the reaction center of *Rb. sphaeroides* at 4.2 K.²¹ For the special pair, electron-exchange interaction is important²² since the Mg···Mg distance of the monomers of the special pair is only 7.2 \AA , which is about 2 \AA shorter than those for the B850 ring (Figure 1). Moreover, rings I of the two BChl molecules of the special pair are close to cofacial and separated by only 3.3 \AA .^{23,24} Such cofacial overlap of rings between neighboring B850 molecules does not occur^{3,4} (Figure 1). The calculations of Sauer et al.,⁵ which neglect electron exchange, yield an effective V for the l-manifold of $\sim -200 \text{ cm}^{-1}$, considerably smaller in magnitude than the value of V deduced above. Given

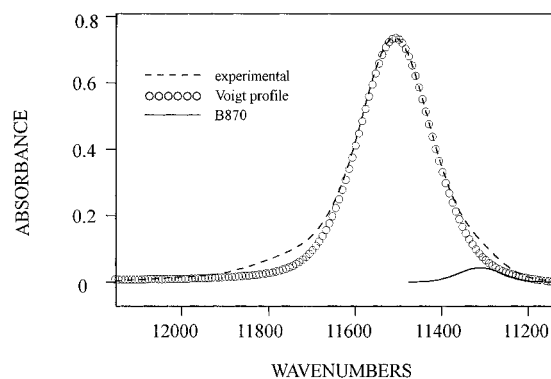


Figure 5. Simulation of the B850 absorption band at 4.2 K. The main part of the B850 absorption band was fit by a Voigt profile (circles, see text) at $11\,504\text{ cm}^{-1}$ with a fwhm of 205 cm^{-1} . The B870 component (solid curve) was obtained by subtracting the Voigt profile from the experimental absorption spectrum (dashed curve).

the differences in structure between the special pair and the dimers of B850, it seems very unlikely that inclusion of electron exchange between neighboring B850 molecules would produce the effective coupling between nearest-neighbor B850 dimers required to have the $j = 0$ exciton level of the l-manifold being located 200 cm^{-1} below the strongly allowed $j = \{1,8\}$ level which determines the maximum of the B850 band.

We propose, therefore, that B870's energetic location is influenced significantly by structural heterogeneity within the B850 ring, i.e., by diagonal and/or off-diagonal energy disorder associated with the dimers of the ring. For theoretical modeling it is necessary to know the integrated intensity of B870 relative to that of the B850 band. To this end, the following procedure was used to obtain the results shown in Figure 5. The position ($11\,300\text{ cm}^{-1}$) and width (120 cm^{-1}) of B870's Gaussian profile were fixed by its ZPH action spectrum (Figure 3). A single Voigt profile was used for the main B850 band at $11\,500\text{ cm}^{-1}$ (Figure 5). The Gaussian and Lorentzian contributions to its width were varied under the constraints that the residual absorption obtained by subtracting the Voigt profile from the experimental spectrum should yield a B870 band as defined above and possess an amplitude consistent with the fact that a ZPH of fractional depth close to 0.5 can be burned at the maximum of B870. Gaussian and Lorentzian widths of 160 and 75 cm^{-1} were found to satisfy these constraints and provide a good fit to the main part of B850 and its low-energy side. That the Gaussian width of 160 cm^{-1} is larger than the 120 cm^{-1} value for B870 is not unreasonable when one realizes that more than one exciton level may well contribute to the main part of the absorption band when energy disorder is taken into account. For example, there are a plethora of ring energy defect patterns which split the degeneracy of the allowed E_1 level.¹⁹ Utilization of a Gaussian width of 120 cm^{-1} led to poor results. The 75 cm^{-1} width corresponds to a relaxation time of 70 fs, which is reasonable given the hole-burning and femtosecond data, cf. Introduction. The intensity of B870 (solid curve) is 3% that of the Voigt profile. However, treating the main part of the B850 band as a single Voigt is an approximation when energy disorder is operative, and the percentage intensity might be as high as 5% (but certainly not 10%). As expected, the fit to the high-energy tail (shoulder) of B850 is poor. This weak but distinct feature of B850 has also been observed in the LH2 complex of *Rb. sphaeroides*.⁷ Although the high-energy tail (shoulder) may be due to vibrational structure, we think this unlikely because of the small Franck-Condon factors for BChl *a* modes near 300 cm^{-1} .^{25,26} That is, the tail absorption is too intense. In this regard, the absorption spectrum shown in Figure 2 is informative since to higher energy of the shoulder and up to the onset of B800 there is no discernible vibronic absorption.

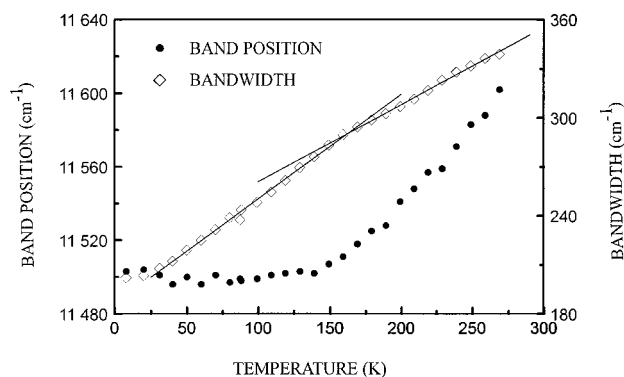


Figure 6. Temperature dependence of the peak position (circles) and width (diamonds) of the B850 band. The solid lines for the broadening data are visual guides. The near-linear band broadening rate is $0.64\text{ cm}^{-1}/\text{K}$ below $\sim 160\text{ K}$ and $0.47\text{ cm}^{-1}/\text{K}$ above 160 K . The uncertainty in the band positions and widths is $\pm 5\text{ cm}^{-1}$.

It is in this region where one might expect to observe more intense modes, e.g., the most intense mode with a frequency of $\sim 750\text{ cm}^{-1}$ and Franck-Condon factor of ~ 0.05 .^{25,26} A more plausible interpretation is that the high-energy tail absorption is due to the l-manifold exciton levels that lie higher than the strongly allowed $j = \{1,8\}$ (E_1) level of Figure 2. (Based on the energy level diagram of Figure 2 the tail absorption could well be due to the $j = \{2,7\}$ level which lies directly above the E_1 level.) Diagonal and/or off-diagonal energy disorder is one mechanism by which the former levels (and the $j = 0$ (A) level) can steal absorption intensity from the latter. Any energy defect model proposed for the B850 ring must be consistent with the just stated weakness of the B870 band; i.e., the presence of diagonal and/or off-diagonal disorder in the excitonic Hamiltonian mixes the zero-order delocalized states associated with perfect cyclic symmetry so that defect models which endow B870 with too much intensity would be suspect. However, slight tilting of the B850 molecular transition dipoles out of the membrane plane (Figure 1) does make the $j = 0$ level of the l-manifold very weakly allowed. This level is polarized perpendicular to the membrane plane. However, the calculations of Sauer et al.⁵ show that the tilting leads to the $j = 0$ (A) level carrying much less than 1% of the intensity of the $j = \{1,8\}$ (E_1) level. (Under perfect cyclic symmetry, the other levels of the l-manifold still remain strictly forbidden.)

To conclude this section, we mention that, prior to hole burning, B870 had been identified by other types of experiments,²⁷⁻²⁹ including time domain at 77 K. (B870 was suggested to be a possible shuttle state for transfer from B850 to B875.) Thus, these works in combination with hole-burning studies convincingly establish the existence of B870 only at cryogenic temperatures. The possibility exists, for example, that the energetic location of B870 relative to the B850 maximum could be different at room temperature. The thermal broadening and band shift data for B850 of the isolated LH2 complex of *Rps. acidophila* shown in Figure 6 indicate that this might be the case. Note first that the B850 band maximum does not shift until $\sim 150\text{ K}$ (approximately glass transition temperature, T_g , of the glycerol:H₂O solvent), at which point it moves to the blue. The thermal broadening data also show a distinct break near 150 K. Up to this break the thermal broadening of B850 can be shown to be consistent with dephasing associated with downward interexciton level relaxation by one-phonon emission (to be published). Similar behavior to that shown in Figure 6 has been observed for *Rb. sphaeroides* and *Rs. molischianum* (results not shown). The weaker thermal broadening of B850 and its blue-shifting for $T > \sim 150\text{ K}$ indicate that formation of the glass leads to an increase in coupling strength between neighboring B850 molecules. The question of the nature of

the associated LH2 structural change is very difficult. At this point we can only mention relevant results for B800. Its thermal broadening and shifting showed *no* break near 150 K. Furthermore, B800's peak position is independent of temperature between 4.2 K and room temperature within experimental uncertainty ($\pm 5 \text{ cm}^{-1}$). The thermal broadening of B800 is weaker than that of B850 below $\sim 150 \text{ K}$ and of a type characteristic of dephasing of isolated monomers in solid hosts, i.e., consistent with the X-ray structure,^{3,4} electronic structure calculations,⁵ and high-pressure studies^{6,8} which indicate that B800–B800 coupling is weak. The above behavior for B800 was also observed for the other two bacterial species. That the B800 band is impervious to glass formation suggests that the structural change of LH2 at T_g is not dramatic although it suffices to affect excitonic interactions within the B850 ring. At present we are attempting to develop a theoretical model for the thermal broadening and shifting of B850 which will lead to an estimate of the extent to which the nearest-neighbor B850–B850 couplings increase upon formation of the glass. This is relevant to electronic structure calculations which use the room temperature X-ray structure and are guided by low-temperature spectroscopic data.

Concluding Remarks

In this paper we have argued that energy disorder (diagonal and/or off-diagonal) in the B850 ring of BChl *a* dimers is important for understanding the location of the lowest exciton level, B870, 200 cm^{-1} below the allowed and adjacent E_1 or $j = \{1,8\}$ level which, to a good approximation, determines the position of the B850 absorption maximum. In the absence of disorder, calculations based on the room temperature X-ray structure of LH2 predict that the $j = 0$ or A level lies 100 cm^{-1} below the E_1 level and is, essentially, forbidden in absorption. It was found that B870, which we associate with the A level, carries about 3% of the total intensity of the B850 absorption band. The presence of both diagonal and off-diagonal energy disorder introduces considerable flexibility to the problem of explaining the energetic location of B870 and understanding of the overall excitonic structure of the B850 ring, especially if correlation in defect patterns is considered. Identifying patterns which produce a significant lowering of B870's energy without endowing it with too much absorption intensity may prove to be challenging. In attempting to do so it will be important to take into account that the temperature dependent data presented here establish that BChl *a*–BChl *a* couplings in the ring strengthen upon formation of the glass. (As mentioned earlier, identification and study of B870 have been restricted to temperatures $\leq 77 \text{ K}$.) An increase in the nearest-neighbor dimer–dimer coupling V reduces the amount of B870 energy lowering required from energy disorder since, in the absence of disorder, the energy gap between the B870 (A) and E_1 levels is $0.46 |V|$ for C_9 symmetry.

That an earlier hole-burning study¹¹ of B870 of *Rps. acidophila* led to it lying 270 cm^{-1} below the B850 absorption maximum deserves some discussion. (A value of 250 cm^{-1} has also been reported for LH2 of *Rb. sphaeroides*.¹⁰) In both of these works, however, the 4.2 K bandwidth of B850 was much broader than 200 cm^{-1} ; cf. Results and Discussion. Very recently, we completed high-pressure hole-burning studies (to be published) of B870 for LH2 samples from *Rb. sphaeroides* which exhibited a narrow bandwidth of 230 cm^{-1} . The zero-phonon action spectrum yielded a displacement of 195 cm^{-1} for B870 below the B850 maximum which within experimental uncertainty is the same as reported here for *Rps. acidophila*. (The LH2 samples were prepared under conditions identical to those used in the present work.) It is apparent, therefore, that

higher sample quality or reduced heterogeneity leads to a reduction in the gap between B870 and the allowed E_1 level. A gap of 200 cm^{-1} would appear to be indicative of a high-quality sample.

Acknowledgment. Research at the Ames Laboratory was supported by the Division of Chemical Sciences, Office of Basic Energy Sciences, U.S. Department of Energy. Ames Laboratory is operated for USDOE by Iowa State University under Contract W-7405-Eng-82. We thank R. J. Cogdell for generously providing us with the samples used in this study and K. Sauer for providing us with a preprint of ref 5 as well as permission to use Figure 1, which is based on one in ref 5.

References and Notes

- (1) Sundström, V.; van Grondelle, R. In *Anoxygenic Photosynthetic Bacteria*; Blankenship, R. E., Madigan, M. T., Baller, C. E., Eds.; Kluwer Academic Publishers: Dordrecht, 1995; p 349.
- (2) Zuber, H.; Cogdell, R. In *Anoxygenic Photosynthetic Bacteria*; Blankenship, R. E., Madigan, M. T., Bauer, C. E., Eds.; Kluwer Academic Publishers: Dordrecht, 1995; p 315.
- (3) McDermott, G.; Prince, S. M.; Freer, A. A.; Hawthornthwaite-Lawless, A. M.; Papiz, M. Z.; Cogdell, R. J.; Isaacs, N. W. *Nature* **1995**, *374*, 517.
- (4) Freer, A.; Prince, S.; Sauer, K.; Papiz, M.; Hawthornthwaite-Lawless, A.; McDermott, G.; Cogdell, R.; Isaacs, N. W. *Structure* **1996**, *4*, 449.
- (5) Sauer, K.; Cogdell, R. J.; Prince, S. M.; Freer, A. A.; Isaacs, N. W.; Scheer, H. *Photochem. Photobiol.* **1996**, *64*, 564.
- (6) Reddy, N. R. S.; Wu, H.-M.; Jankowiak, R.; Picorel, R.; Cogdell, R. J.; Small, G. J. *Photosynth. Res.* **1996**, *48*, 277.
- (7) Reddy, N. R. S.; Small, G. J.; Seibert, M.; Picorel, R. *Chem. Phys. Lett.* **1991**, *181*, 391.
- (8) Wu, H.-M.; Savikhin, S.; Reddy, N. R. S.; Jankowiak, R.; Cogdell, R. J.; Struve, W. S.; Small, G. J. *J. Phys. Chem.* **1996**, *100*, 12022.
- (9) Karrasch, S.; Bullough, P. A.; Ghosh, R. *EMBO J.* **1995**, *14*, 631.
- (10) Reddy, N. R. S.; Picorel, R.; Small, G. J. *J. Phys. Chem.* **1992**, *96*, 6458.
- (11) Reddy, N. R. S.; Cogdell, R. J.; Zhao, L.; Small, G. J. *Photochem. Photobiol.* **1993**, *57*, 35.
- (12) Savikhin, S.; Struve, W. S. *Biophys. J.* **1994**, *67*, 2002.
- (13) Savikhin, S.; Struve, W. S. *Chem. Phys.* **1996**, *210*, 91.
- (14) Cogdell, R. J.; Hawthornthwaite, A. M. In *The Photosynthetic Reaction Center*; Deisenhofer, J., Norris, J. R., Eds.; Academic Press: San Diego, 1993; Vol. 1, p 23.
- (15) Chang, H. C.; Jankowiak, R.; Reddy, N. R. S.; Small, G. J. *Chem. Phys.* **1995**, *197*, 307.
- (16) Small, G. J. *Chem. Phys.* **1995**, *197*, 239.
- (17) Shu, L.; Small, G. J. *J. Opt. Soc. Am.* **1992**, *B9*, 724.
- (18) Koepke, J.; Hu, X.; Muenke, C.; Schulten, K.; Michel, H. *Structure* **1996**, *4*, 581.
- (19) Wu, H.-M.; Small, G. J. To be published.
- (20) Pearlstein, R. M.; Zuber, H. In *Antennas and Reaction Centers of Photosynthetic Bacteria*; Springer Ser. Chem. Phys. **42**.
- (21) Tang, D.; Jankowiak, R.; Hayes, J. M.; Small, G. J.; Tiede, D. M. In *22nd Jerusalem Symposium on Quantum Chemistry and Biochemistry: Perspectives in Photosynthesis*; Jortner, J., Pullman, B., Eds.; Kluwer: Dordrecht, 1990; p 99.
- (22) Thompson, M. A.; Schenter, G. K. *J. Phys. Chem.* **1995**, *99*, 6374 and references therein.
- (23) Chang, C. H.; Tiede, D.; Tang, J.; Smith, U.; Norris, J.; Schiffer, M. *FEBS Lett.* **1986**, *205*, 82.
- (24) Ermler, U.; Fritzsche, G.; Buchanan, S. K.; Michel, H. *Structure* **1994**, *2*, 925.
- (25) Renge, I.; Muring, K.; Avarmaa, R. *J. Lumin.* **1987**, *37*, 207.
- (26) Gillie, J. K.; Small, G. J.; Golbeck, J. H. *J. Phys. Chem.* **1989**, *93*, 1620.
- (27) Bolt, J.; Sauer, K. *Biochim. Biophys. Acta* **1979**, *546*, 54.
- (28) Kramer, H. J. M.; Pennoyer, J. D.; van Grondelle, R.; Westerhuis, W. H. J.; Neidermann, R. A.; Ames, J. *Biochim. Biophys. Acta* **1984**, *767*, 335.
- (29) van Dorssen, R. J.; Hunter, C. N.; van Grondelle, R.; Korenhof, A. H.; Ames, J. *Biochim. Biophys. Acta* **1988**, *932*, 179.